DOI: http://dx.doi.org/10.12989/was.2007.10.2.209
Wind and Structures, Vol. 10, No. 2 (2007) 209-214

Technical Note

Simulation study of SRS-based adaptive feedforward vibration control

Fujun Peng† and Ming Gu‡

State Key Laboratory for Disaster Reduction in Civil Engineering, Tongji University, Shanghai, 200092, P. R. China

Hans-Jürgen Niemann‡

Boundary Layer Wind Tunnel Laboratory, Ruhr-Universität Bochum, D-44780 Bochum, Germany

(Received November 8, 2004, Accepted October 31, 2006)

1. Introduction

Active structural control has turned out to be an effective mean to reduce wind-induced response, and a number of control algorithms have been developed. However, most of these algorithms are generally based on an accurate model of the structure to be controlled (Housner, *et al*. 1997, Yang, *et al*. 2004). In this paper, Sinusoidal Reference Strategy is developed for the adaptive feedfowrd vibration control and some properties of the control system are discussed. Numerical simulations are conducted on reducing wind-induced vibration of Jin Mao building. The results show that remarkable vibration reduction can be obtained, and the control system is quite robust to dynamic uncertainties and modelling errors.

2. Development of sinusoidal reference strategy

The block diagram of the conventional adaptive feedforward control is shown in Fig. 1 (Elliott 2001). $\mathbf{P_1}$ is the transfer property of the controlled structure from the external excitation to the sensor.

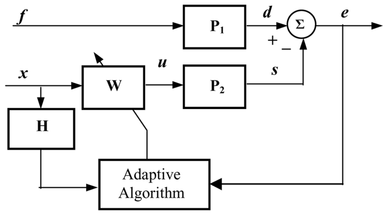

Fig. 1 Block diagram of adaptive feedforward control

† Professor, Corresponding Author, E-mail: pfj_tj@yahoo.com
‡ Professor

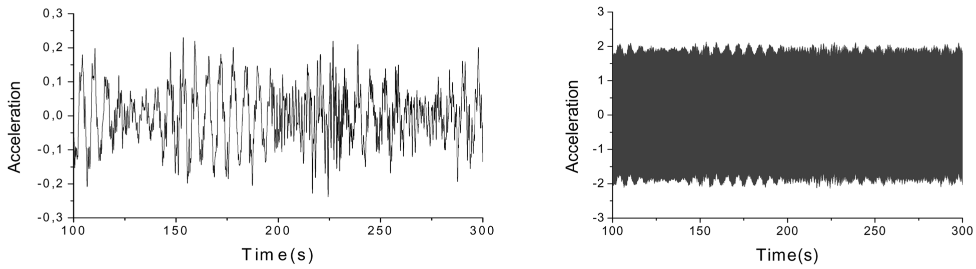

(a) Original uncontrolled response (b) Mixed response

Fig. 2 Sample of typical uncontrolled response and mixed response

$\mathbf{P_2}$ is the transfer property from the control force to the sensor. **H** is the N-order identified FIR (Finite Impulse Response) model of $\mathbf{P_2}$. **W** is a FIR controller. $\boldsymbol{x}$ is the reference signal. $\boldsymbol{f}$ is the external excitation. $\boldsymbol{d}$ is the response to the external excitation. $\boldsymbol{u}$ is the control force. $\boldsymbol{s}$ is the response to the control force. $\boldsymbol{e}$ is the error response, i.e., the sum of the responses to external excitation and control force. The adaptive algorithm adjusts controller parameters in real time according to the error responses measured by sensors, and makes these parameters converging to their optimal values.

2.1. Introducing additional sinusoidal signal into adaptive feedforward control

From the vibration cancellation point of view, one of the difficulties in reducing wind-induced vibration of super-tall buildings comes from the violent variation of the uncontrolled response, a typical sample of which is shown in Fig. 2(a). As a solution, a higher frequency sinusoidal signal is added here to the original uncontrolled response and the mixed response is regarded as the objective response to be controlled. The mixed response is shown in Fig. 2(b). Considering the relatively alleviated variation of the amplitude, one can expect intuitively that better results may be obtained than controlling the original response directly.

The mixed response is dominated by the additional sinusoidal signal, therefore, the reference signal of the adaptive feedforward control can be determined as a sinusoidal signal with the same frequency. Then the block diagram of adaptive feedforward control system evolves into Fig. 3, where, **K** is a proportional coefficient, used for adjusting the amplitude of the additional sinusoidal signal. In order to improve tracking capability of the control system, filtered-x RLS algorithm is used here. The recursive formulae can be expressed as:

$$H = [h_1\ h_2 \cdots h_N] \tag{1}$$

$$W(n) = [w_1\ w_2 \cdots w_N] \tag{2}$$

$$x(n) = A\sin(n\omega\Delta t) \tag{3}$$

$$X_N(n) = [x(n)\ \ x(n-1) \cdots x(n-N+1)] \tag{4}$$

$$y(n) = X_N(n)H^T \tag{5}$$

$$Y_N(n) = [y(n)\ \ y(n-1) \cdots y(n-N+1)] \tag{6}$$

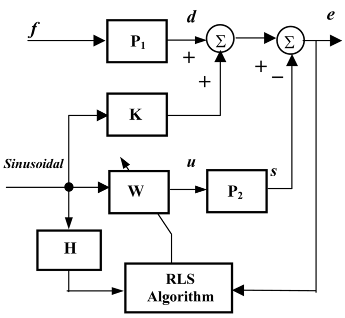

Fig. 3 Block diagram of adaptive feedforward control for reducing mixed response

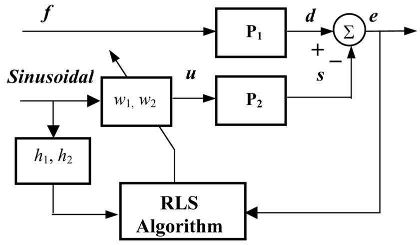

Fig. 4 Block diagram of SRS-based adaptive feed-forward control

$$P_N(n) = C_{NN}(n-1)Y_N^T(n) \tag{7}$$

$$C_{NN}(n) = \frac{1}{\lambda}\left[C_{NN}(n-1) - \frac{P_N(n)P_N^T(n)}{\lambda + Y_N(n)P_N(n)}\right] \tag{8}$$

$$W(n) = W(n-1) + P_N^T(n)/(\lambda + Y_N(n)P_N(n))e(n) \tag{9}$$

$$u(n) = X_N(n)W^T(n) \tag{10}$$

where, n is time index, λ is forgetting factor, Δt is time interval of control update.

2.2. Removing the negative influence of the additional sinusoidal signal

In the control system shown in Fig. 3, the control signal consists of two components: one corresponds to the uncontrolled response and the other corresponds to the additional sinusoidal signal. The former is the desired component for reducing the original uncontrolled response. But the latter will lead additional undesired response if it applies to the structure directly. In order to remove this negative effect, Eq. (9) is investigated in more detail. It can be re-written as:

$$W_1(n) + W_2(n) = W_1(n-1) + W_2(n-1) + P_N^T(n)/(\lambda + Y_N(n)P_N(n))(e_1(n) + e_2(n)) \tag{11}$$

where, $W_1(n)$ and $W_2(n)$ are two components of the controller that correspond to the two control signal components, respectively. $e_1(n)$ and $e_2(n)$ are error components corresponding to the original uncontrolled response and the additional signal. When $W_2(n)$ converges sufficiently, $W_2(n)$ is approximately identical to $W_2(n-1)$, and $e_2(n)$ is much less than $e_1(n)$ and thus can be neglected in Eq. (11). So we have:

$$W_1(n) = W_1(n-1) + P_N^T(n)/(\lambda + Y_N(n)P_N(n))e_1(n) \tag{12}$$

Eq. (12) shows that the recursive computation of $W_1(n)$ is independent of $W_2(n)$ and the amplitude of the additional sinusoidal signal. Therefore the proportional coefficient **K** in Fig. 3 can be set as zero, thus $W_2(n)$ becomes definitely an zero-vector. So the negative influence of the additional signal is removed and the control signal contains only the desired component. The block diagram of SRS-based adaptive feeforward control is shown in Fig. 4.

2.3. Characteristics of SRS-based adaptive feedforward control

It seems that Fig. 4 is very similar to the conventional adaptive feedforward control. But in fact it has some unique characteristics: (1) Its reference signal is definitely selected as a sinusoid, which frequency is much higher than all the dominant modal frequencies of the controlled structure. This is quite different from the conventional principle for selecting reference signal. (2) The orders of FIR model and controller are definitely selected as 2, since the reference signal is only of 2-order persistent excitation. Theoretically, this is the smallest size for them. Such a small size can remarkably reduce the computation amount during per control update interval, and thus make the algorithm to be implemented more easily. (3) The identification of FIR model is offline conducted using adaptive identification method with the same sinusoid as reference signal. The updating rate is selected the same as that for controlling. Only the dominant modes are included through using modal filters. Such a modelling method means that the two parameters of FIR model only reflect amplitude and phase properties at a relatively high frequency point. It is well known that a vibration system appears to be nearly inertial under high frequency excitations, and the amplitude and phase properties are not sensitive to the fluctuation of damping and stiffness of vibration system. The present modelling method, therefore, is helpful to improve the robustness of the whole control system.

3. Numerical simulations

The simulation is conducted on reducing wind-induced vibrations of Jin Mao Building, 420 m high, located in Shanghai, China. It is modelled as a cantilever beam with only the first three modes considered, and their natural frequencies are 0.16148 Hz, 0.66363 Hz and 1.43068 Hz, respectively. The first three modal masses are 42323T, 33452T and 31114T. Modal damping ratio is set 0.15 for all the first three modes. The terrain condition is considered as category D. The exponent α of the average wind profile is 0.3 and the corresponding gradient height is 450 m according to Chinese code. The 10-year return period wind speed at the gradient height under Terrain D is 46.2 m/s. An AMD is considered as the actuator, installed on the top of the building, which weighs 423T, about 1% of the first modal mass of Jin Mao Building. First two modal acceleration responses at the top of the buildings are to be controlled. In order to evaluate the robustness of the controller, only stiffness uncertainty of building is considered since the active controllers are not sensitive to the uncertainty in damping. Stiffness uncertainties are assumed in 7 cases from 15% to −15% by multiplying 1.0724, 1.0488, 1.0247, 1.0000, 0.9747, 0.9487 and 0.9220 to the first three modal frequencies, respectively. The controller is designed below, and the same controller is applied to all

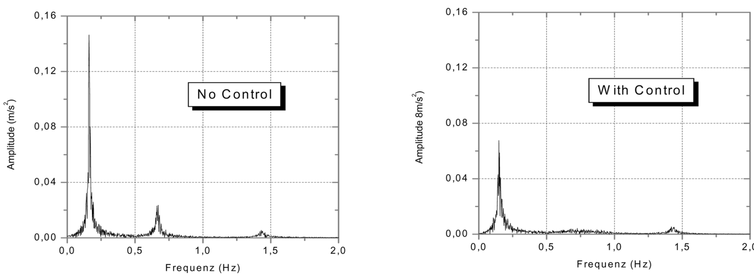

(a) (b)

Fig. 5 Frequency spectra of uncontrolled and controlled response of zero-uncertainty building the 7 cases: Control updating rate $f=75$ Hz; Reference signal ***Sinusoidal*** $=\sin(2\pi\times 16.148\times n/f)$, n is time index; Forgetting factor $\lambda=0.1$; Identified model $[\boldsymbol{h}_1, \boldsymbol{h}_2]=[8.60\times 10^{-8}, -1.34\times 10^{-10}]$; Initialization for $n=0$: $[\boldsymbol{w}_1, \boldsymbol{w}_2]=[0.0, 0.0]$, $C_{NN}(n)=dia(1.0\times 10^{12}, 1.0\times 10^{12})$.

Fig. 5 shows the frequency spectra of uncontrolled and controlled accelerations of zero-uncertainty building. The corresponding frequency spectra of controller parameters and control force are presented in Fig. 6. Control efficiencies in peak and RMS values in all 7 cases are shown in Table 1. In order to evaluate the effect of forgetting factor, simulations are conducted on controlling zero-uncertainty building using different forgetting factors in the controller, while keep other control system parameters same as before. Results are shown in Table 2.

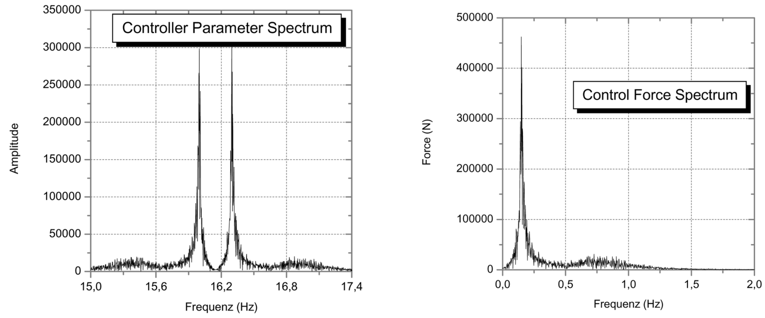

(a) (b)

Fig. 6 Frequency spectra of the first controller parameter and control force for controlling zero-uncertainty building

Table 1 Control efficiency under different stiffness uncertainty

Uncertainty (%)	No control (m/s^2)		With control (m/s^2)		Control efficiency (%)	
	Peak	RMS	Peak	RMS	Peak	RMS
15	56.735	20.987	35.524	11.737	37.386	44.075
10	61.318	21.819	34.114	11.722	44.365	46.276
5	65.381	23.096	35.510	11.711	45.687	49.294
0	66.527	22.182	34.749	11.829	47.767	46.673
-5	66.306	22.652	35.267	12.076	46.812	46.689
-10	68.097	23.186	36.849	12.310	45.888	46.908
-15	59.637	23.774	37.451	12.347	37.202	48.065

Table 2 Control efficiency under different forgetting factor

Forgetting factor	No control (m/s^2)		With control (m/s^2)		Control efficiency (%)	
	Peak	RMS	Peak	RMS	Peak	RMS
0.10	66.527	22.182	34.749	11.829	47.767	46.673
0.15	66.527	22.182	34.636	11.835	47.937	46.646
0.20	66.527	22.182	35.054	11.974	47.309	46.019
0.25	66.527	22.182	35.454	12.130	46.707	45.316
0.30	66.527	22.182	35.931	12.309	45.990	44.509
0.35	66.527	22.182	36.502	12.512	45.132	43.594
0.40	66.527	22.182	36.855	12.745	44.601	42.544

Comparing the frequency spectra of the uncontrolled and controlled accelerations shown in Fig. 5, one can find that the first two modal responses are reduced effectively. Fig. 6(a) shows that frequency spectra of controller parameters contain four peaks, two of them are corresponding to the sum of reference signal frequency and first two modal frequencies, and the other two are corresponding to the subtraction of reference signal frequency and first two modal frequencies. The control signal, which is a convolution of the reference sinusoidal signal and controller parameters, contains two dominant frequency components, shown in Fig. 6(b), corresponding to first two modal frequencies of Jin Mao building. The results in Table 1 show that control efficiencies corresponding to different uncertainties do not change much, which demonstrates that the control system has good robustness. Comparing results in Table 2, we can see that lower forgetting factor is helpful to improve control efficiency.

4. Conclusions

Sinusoidal Reference Strategy is developed in this paper. Comparing with the conventional adaptive feedforward control, the new strategy has some superior properties in constructing reference signal, reducing the orders of the FIR model and controller, taking less computation, and having better tracking capability etc. Numerical simulations are conducted and remarkable reductions are obtained. The results also show good robustness of the present strategy.

Acknowledgements

The authors gratefully acknowledge supports of the National Science Foundation for Outstanding Youth, Foundation for University Key Teacher by the Ministry of Education, and National Natural Science Foundation (59895410). This work is also partially supported by Alexander von Humboldt Foundation, which is gratefully acknowledged.

References

Elliott, S. J. (2001), *Signal Processing for Active Control*. Academic Press, London.

Housner, G. W., Bergman, L. A., *et al.* (1997), "Structural control: Past, present, and future", *J. Eng. Mech.*, **123**(9), 897-971.

Yang, J. N., Lin, S., and Jabbari, F. (2004), "Linear multiobjective control strategies for wind-excited buildings", *J. Eng. Mech.*, **130**(4), 471-477.

CC